Supplementary Figure 1.

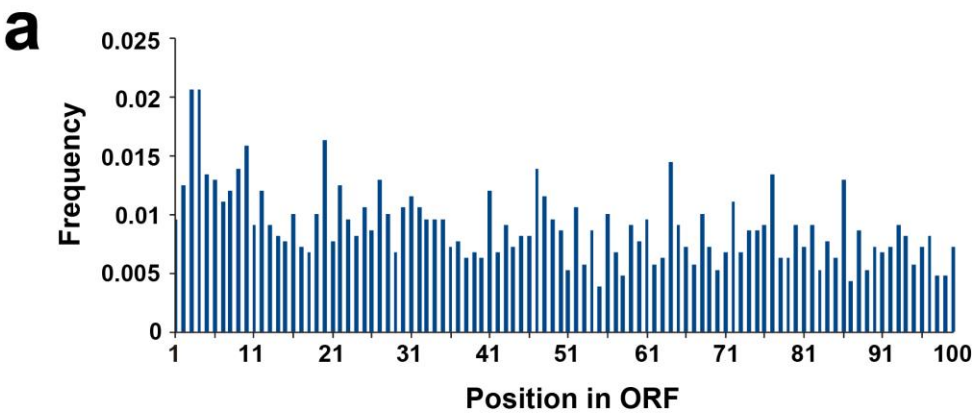

b

pncA **(nicotiamidase/pyrazinamidase)**

AUG CCC CCU CGC GCC
M P P R A

mutH **(methyl-directed mismatch repair protein)**

AUG UCC CAA CCU CGC CCA CUG CUC UCU CCU CCC GAA
M S Q P R P L L S P P E

sfsA **(DNA-binding transcriptional regulator)**

AUG GAA UUU UCU CCU CCC CUA
M E F S P P L

rutD **(pyrimidine utilization protein D)**

AUG AAA CUU UCA CUC UCA CCU CCC CCU UAU
M K L S L S P P P Y

aldB **(acetaldehyde dehydrogenase)**

AUG ACC AAU AAU CCC CCU UUC
M T N N P P F

fumA **(fumarase A)**

AUG UCA AAC AAA CCC UUU
M S N K P F

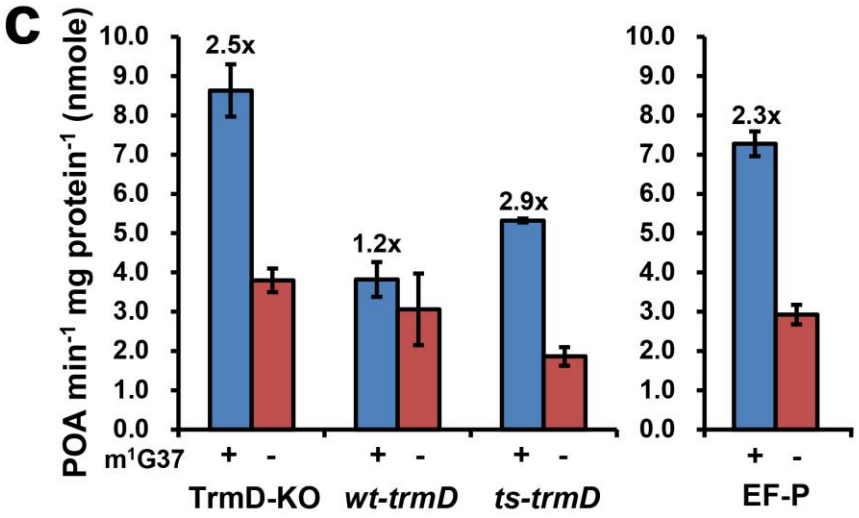

Supplementary Figure 1. Translation of naturally occurring CC[C/U]-[C/U] sequences in *E. coli*.

a. The frequency of occurrence of CC[C/U]-[C/U] in *E. coli* K12 protein coding genes. The frequency is calculated for each codon position, against the total sense codons, up to the first 100 codons in *E. coli*. The number of occurrences up to the first 100 codons accounts for ~80% of the total number of occurrences in the entire 4,288 *E. coli* protein coding genes. **b.** Examples of *E. coli* genes containing CC[C/U]-[C/U] near the AUG initiation codon and the decoded amino acid residues. **c.** Enzyme activity of the endogenous *E. coli* pyrazinamidase nicotiamidase-pyrazinamidase (PZase) in cell lysates. The activity was monitored by following the production of pyrazinoic acid (POA) in the presence or absence of synthesis of m^1G37 or expression of EF-P. The deficiency of m^1G37 and EF-P was created in *trmD-KO* and *efp-KO* strains. As a second method to test the deficiency of m^1G37, the *ts-trmD-S88L* strain[1] and the isogenic *wt-trmD* strain were used. The m^1G37+ data (blue bars) were collected from cells grown at 30 °C whereas the m^1G37- data (red bars) were from cells grown at 43 °C. The fold-increase in the enzyme activity upon expression of m^1G37 or EF-P is shown for each strain. Each value represents the average of at least three independent measurements and error bars are SD. Calculated P values based on the data were below 0.05.

Supplementary Figure 2.

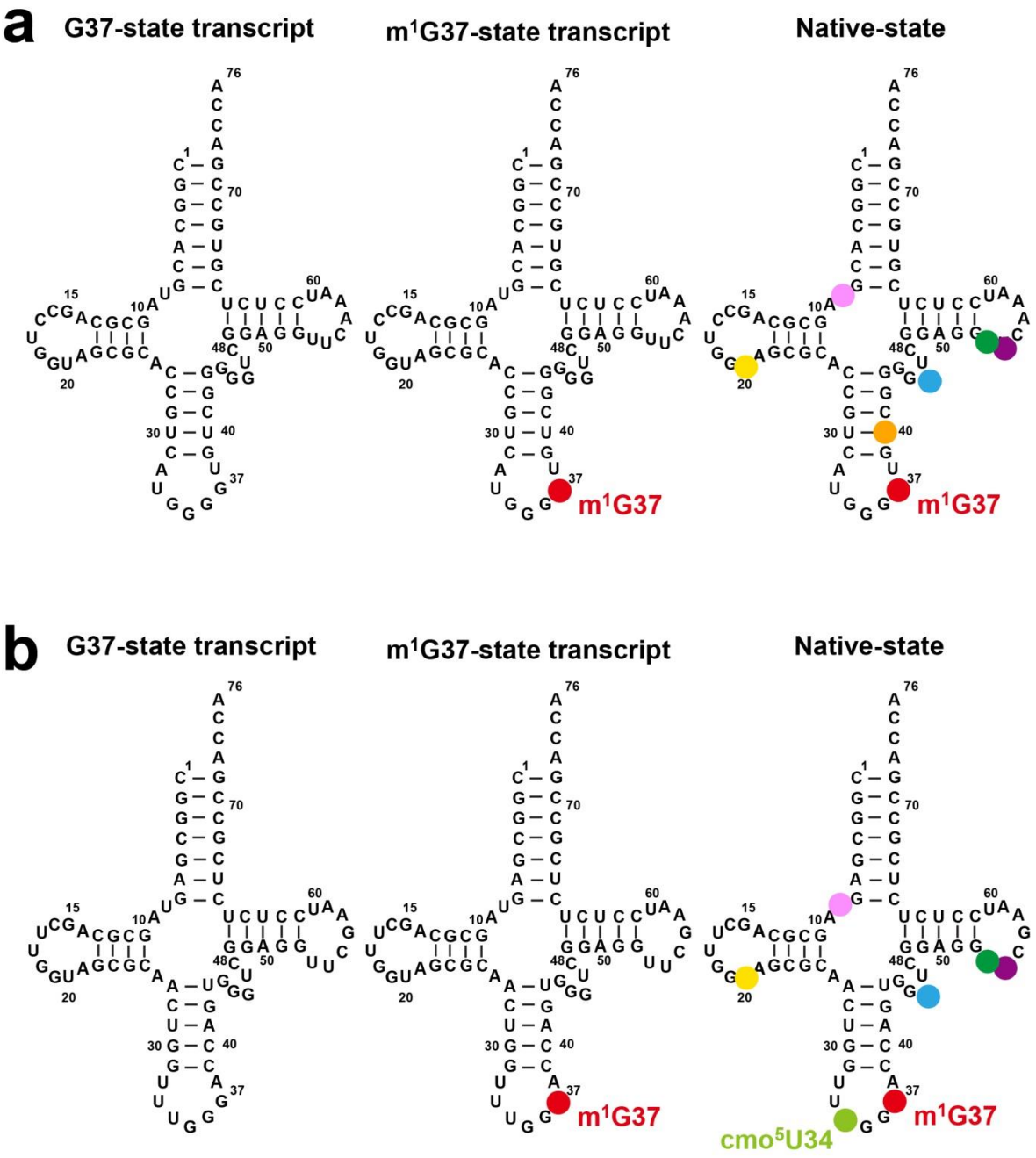

Supplementary Figure 2. Sequence and cloverleaf structure of *E. coli* (a) tRNA$^{Pro/GGG}$ and (b) tRNA$^{Pro/UGG}$ in the three states.

Note that natural modifications s^{4}U9, D20, cmo^{5}U34, m^{1}G37, ψ40, m^{7}G46, T54, and ψ55 in the native state are represented by pink, yellow, light green, red, blue, dark green, and purple dots,

respectively. These modifications are deduced from the known modifications of GGG and UGG isoacceptors in *Salmonella typhimurium*.

Supplementary Figure 3.

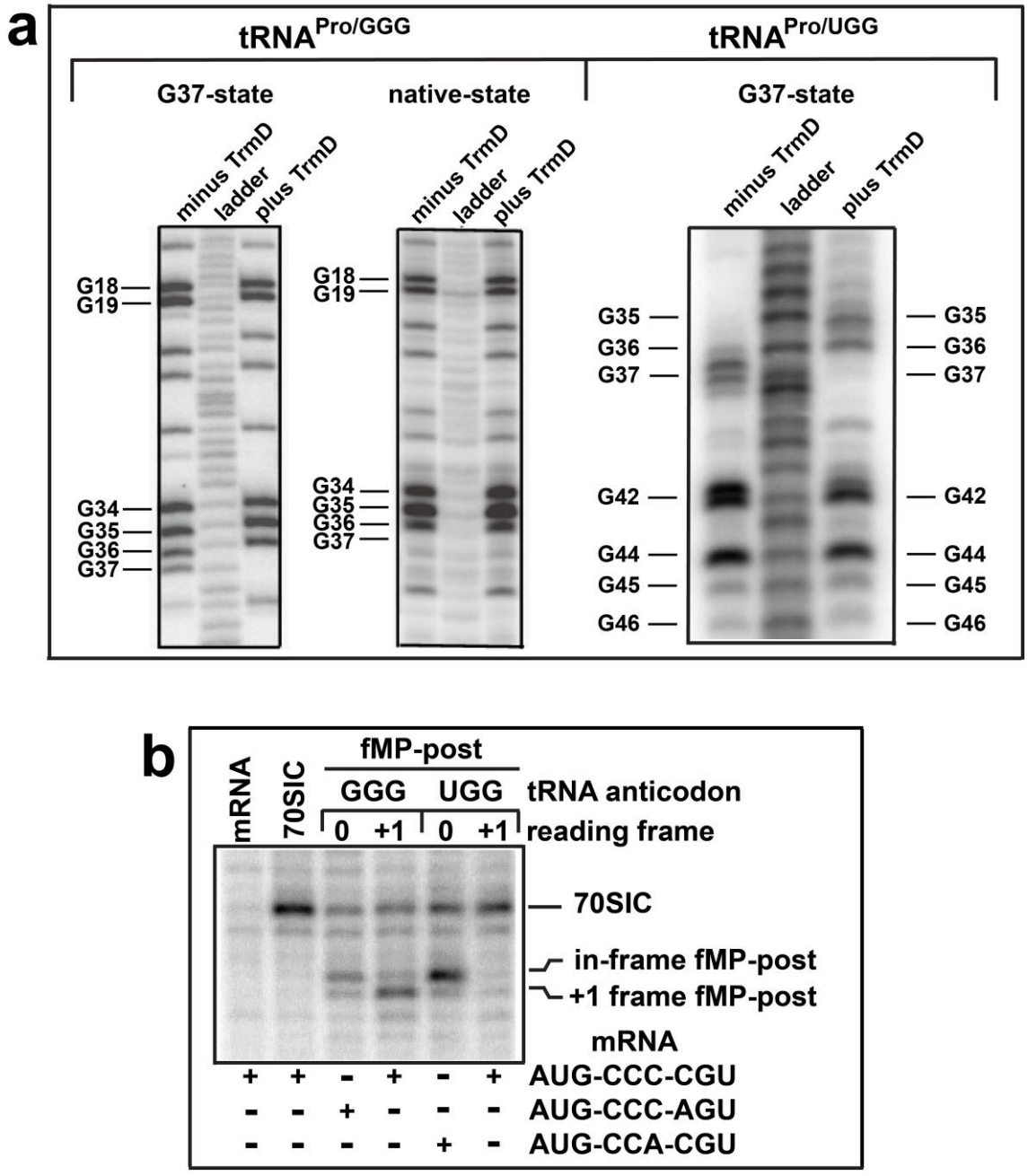

Supplementary Figure 3. Footprint of tRNA^{Pro} and toeprint of fMP-post-translocation complexes.

a. RNase T1 analysis. Native and transcript tRNA$^{Pro/GGG}$ as well as transcript tRNA$^{Pro/UGG}$ were 3'-end labeled with ^{32}P and digested with RNase T1 under conditions giving approximately one nick per molecule. Digested tRNAs were electrophoresed in a denaturing 12% PAGE/7M

urea gel along with a ladder generated by alkaline hydrolysis. Cleavage at G37 was observed for G37-state $tRNA^{Pro}$ without TrmD reaction (minus), but was not observed after the TrmD reaction (plus). Neither was cleavage observed in the native-state $tRNA^{Pro}$, with or without TrmD reaction. **b.** Toeprint analysis. fMP-post-translocation complexes were formed with unlabeled fMet-$tRNA^{fMet}$ on three 96-mer mRNAs, whose starting coding sequences are indicated below the phosphorimage. Toeprinting was performed with minor variations of published work[2]. Arrest of primer extension by the ribosome generated a toeprint +15 nucleotides downstream of the first nucleotide of the codon at the P-site. Banding was resolved on a 9% sequencing gel. Relative to a 70SIC, primer extension of a stalled fMP-post-translocation complex formed with G37-state $tRNA^{Pro/GGG}$ on a non-slippery CCC-A sequence gave a product of 3 nucleotides shorter, corresponding to the in-frame complex. In contrast, primer extension of a similar fMP-post-translocation complex formed on the slippery CCC-C sequence gave a product of 4 nucleotides shorter, corresponding to the +1-frame complex. When an fMP-post-translocation complex was formed with G37-state $tRNA^{Pro/UGG}$, a stable in-frame complex was formed when the coding sequence was CCA-C but no complex was detected with the slippery CCC-C sequence, possibly due to drop-off of the tRNA during analysis.

Supplementary Figure 4.

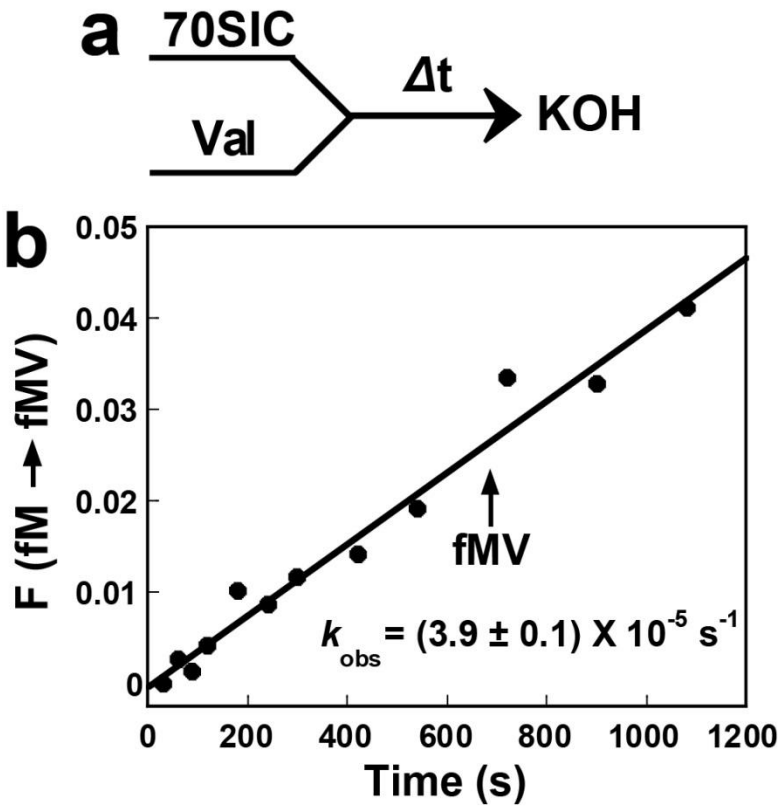

Supplementary Figure 4. Misincorporation of $tRNA^{Val/UAC}$ is a rare event.

a. A 70SIC programmed with the mRNA (AUG-CGU-UGA) encoding the fMR dipeptide was incubated with the ternary complex of $tRNA^{Val/UAC}$ (anticodon presented 5' to 3'). Note that the U in the anticodon of this native-state $tRNA^{Val}$ is modified to cmo^5U, which can base pair to the wobble U of the GUU codon[3]. **b.** Kinetics of synthesis of fMV, due to mispairing of $tRNA^{Val}$ to the in-frame Arg CGU codon or cognate pairing to the out-of-frame Val GUU codon, was slow relative to the shifting of $tRNA^{Pro}$ into the +1-frame (see **Fig. 2** of the main text).

Supplementary Figure 5.

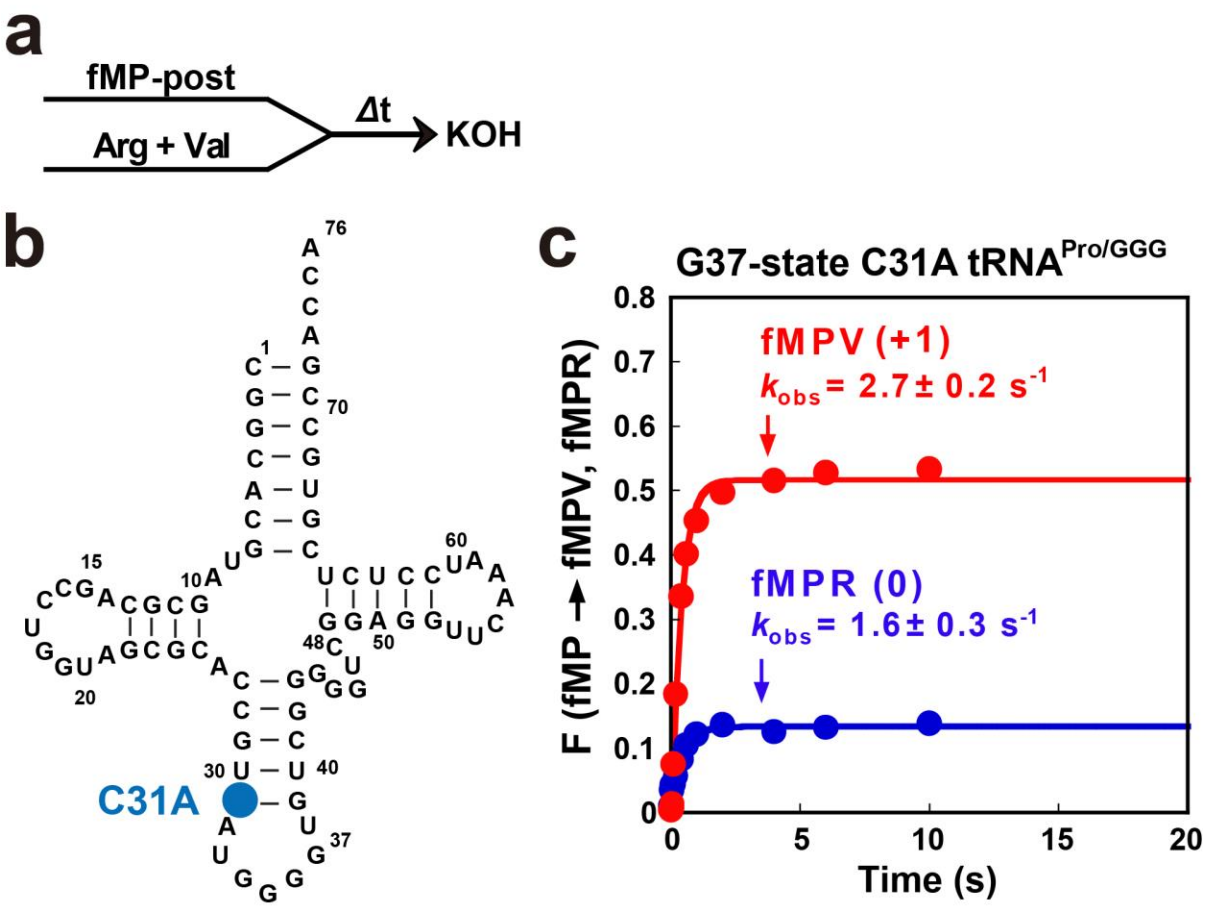

Supplementary Figure 5. The C31A mutation in tRNA$^{Pro/GGG}$ promotes +1FS errors in a stalled post-translocation complex.

a. Kinetic scheme for monitoring +1FS by G37-state C31A tRNA$^{Pro/GGG}$ in a stalled fMP-post-translocation complex programmed by the AUG-CCC-CGU-U sequence. The post-translocation complex was rapidly mixed with the ternary complex of tRNA^{Arg} or tRNA^{Val}. Reaction aliquots were quenched with KOH and peptides were resolved on electrophoretic TLC. **b**. The C31A substitution disrupts the 31-39 base pair of the tRNA anticodon stem. **c.** Kinetics of synthesis of the in-frame fMPR (in blue) and +1-frame fMPV (in red) were similar in rate but with fMPV being the major product. The corresponding G31A mutation in G37-state tRNA$^{Pro/UGG}$ also enhanced +1FS in a stalled post-translocation complex (data not shown).

Supplementary Figure 6

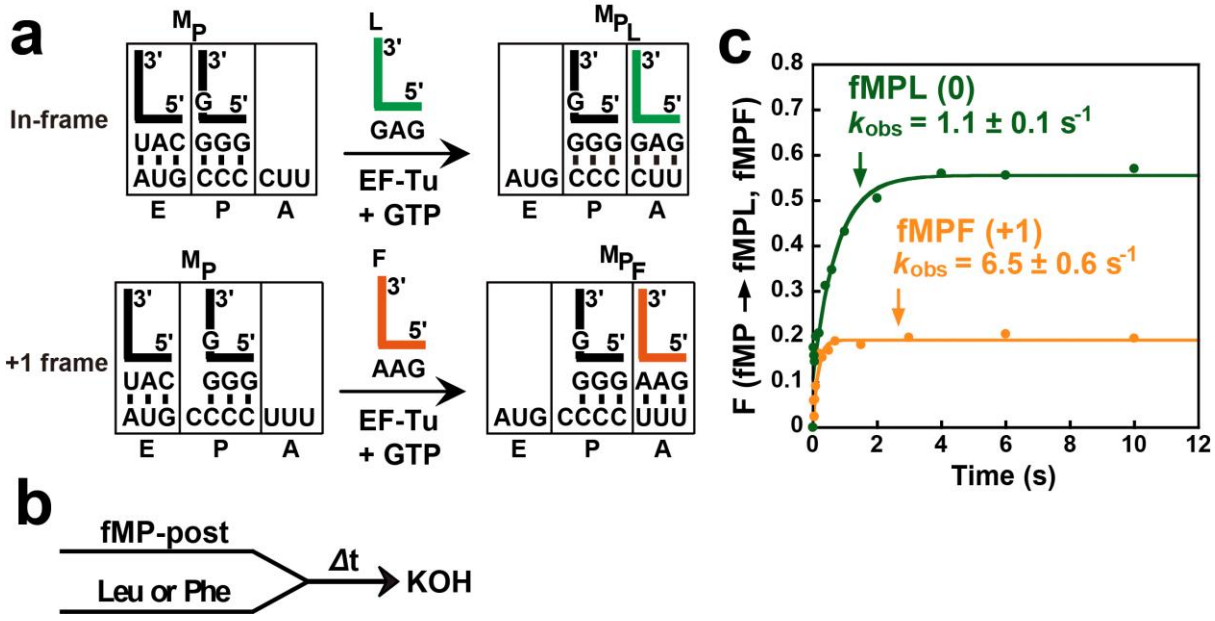

Supplementary Figure 6. Shifting of G37-state tRNA$^{Pro/GGG}$ in the P-site of a stalled post-translocation complex in a different sequence context.

a. Diagram of an fMP-post-translocation complex programmed by AUG-CCC-CUU-U, where the G37-state fMP-tRNA$^{Pro/GGG}$ in the P-site can pair to the slippery CCC-C in the 0-frame or +1-frame. These pairing states determine the identity of the next incoming tRNA based on the sequence context downstream from the CCC-C run. In-frame pairing of tRNA^{Pro} leads to the synthesis of fMPL while +1-frame pairing leads to the synthesis of fMPF. **b.** Reaction scheme for monitoring fMPL and fMPF formation. The stalled fMP-post-translocation complex was rapidly mixed with ternary complexes of tRNA^{Leu} or tRNA^{Phe}. Reaction aliquots were quenched with KOH and analyzed by electrophoretic TLC. **c.** Kinetics of formation of fMPL (in green) and fMPF (in orange). The in-frame tripeptide dominated in total products, although the kinetics of product synthesis was somewhat slower relative to the +1-frame tripeptide. The close similarity in results between this sequence context and that in **Fig. 2b** indicates that sequences downstream of the CCC-C run do not affect +1-frame pairing of tRNA$^{Pro/GGG}$.

Supplementary Figure 7

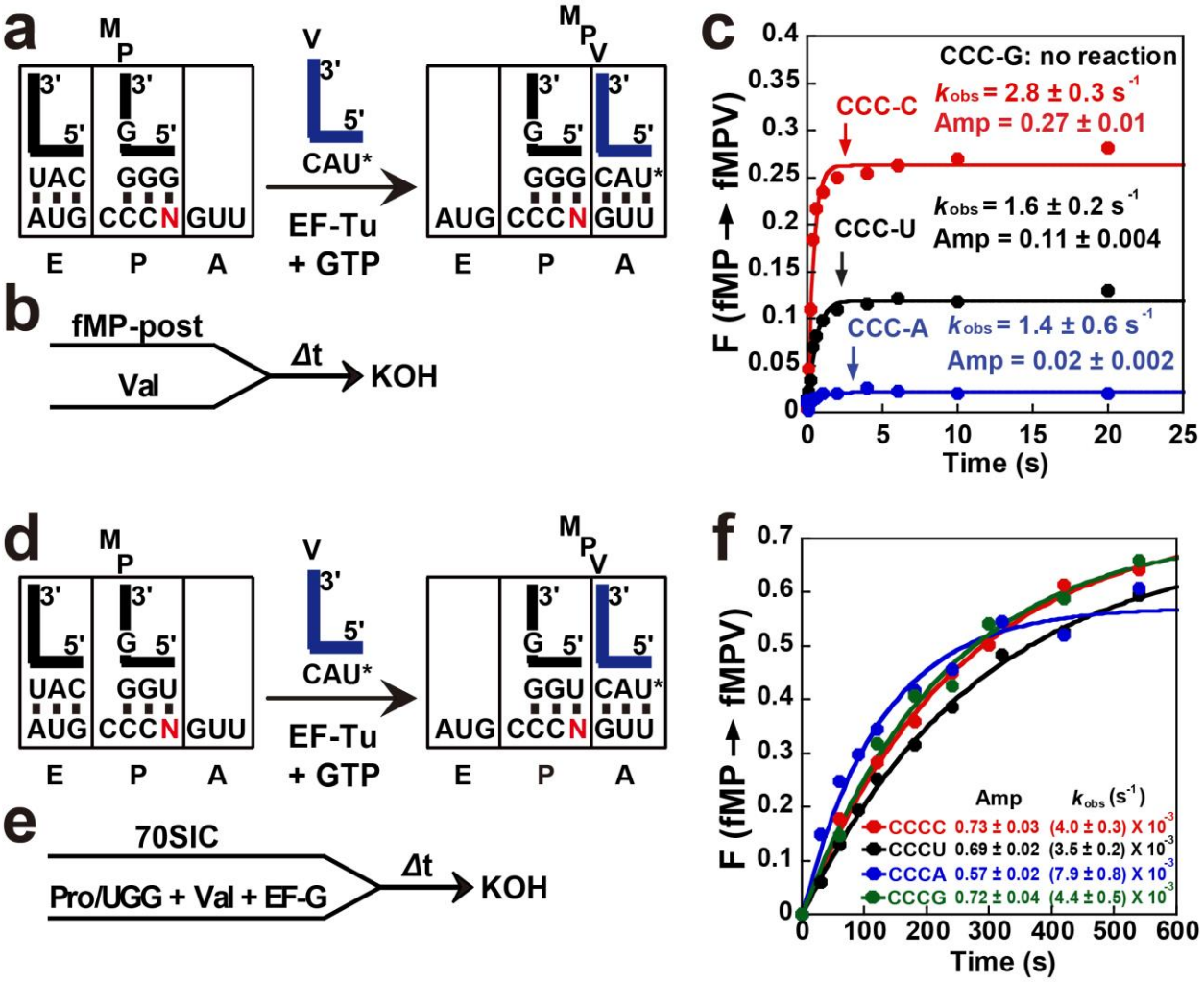

Supplementary Figure 7. G37-state tRNA$^{Pro/GGG}$ and tRNA$^{Pro/UGG}$ exhibit different +1FS profiles when decoding CCC-N sequences under non-competitive conditions.

a-**c.** Stalled post-translocation complexes bearing fMP-tRNA$^{Pro/GGG}$ in the P-site were prepared using four different mRNA sequences (AUG-CCC-NGU-U where N = A, U, G, or C). Formation of the +1FS product fMPV was monitored in the presence of tRNA^{Val} by quenching reaction aliquots with KOH prior to analysis by electrophoretic TLC. The extent of +1FS supported by each mRNA was dependent upon the stability of the C-N wobble pair in the frameshifted state. **d**-**f.** A similar analysis was carried out with tRNA$^{Pro/UGG}$ in concerted reactions

starting out with 70SIC. All four mRNAs supported similar levels of +1FS, as would be expected for a tRNA that is mismatched at the wobble position in the in-frame state. The high levels of +1FS indicate reversibility between the in-frame and +1-frame pairing states of $tRNA^{Pro/UGG}$ in the post-translocation complex. This propensity to +1FS suggests that $tRNA^{Pro/UGG}$ is highly prone to shifting whenever it encounters a CCC-N sequence. Among the total sense codons in *E. coli*, the CCC-N sequences occur 8861 times (at a frequency of 0.55%).

Supplementary Figure 8.

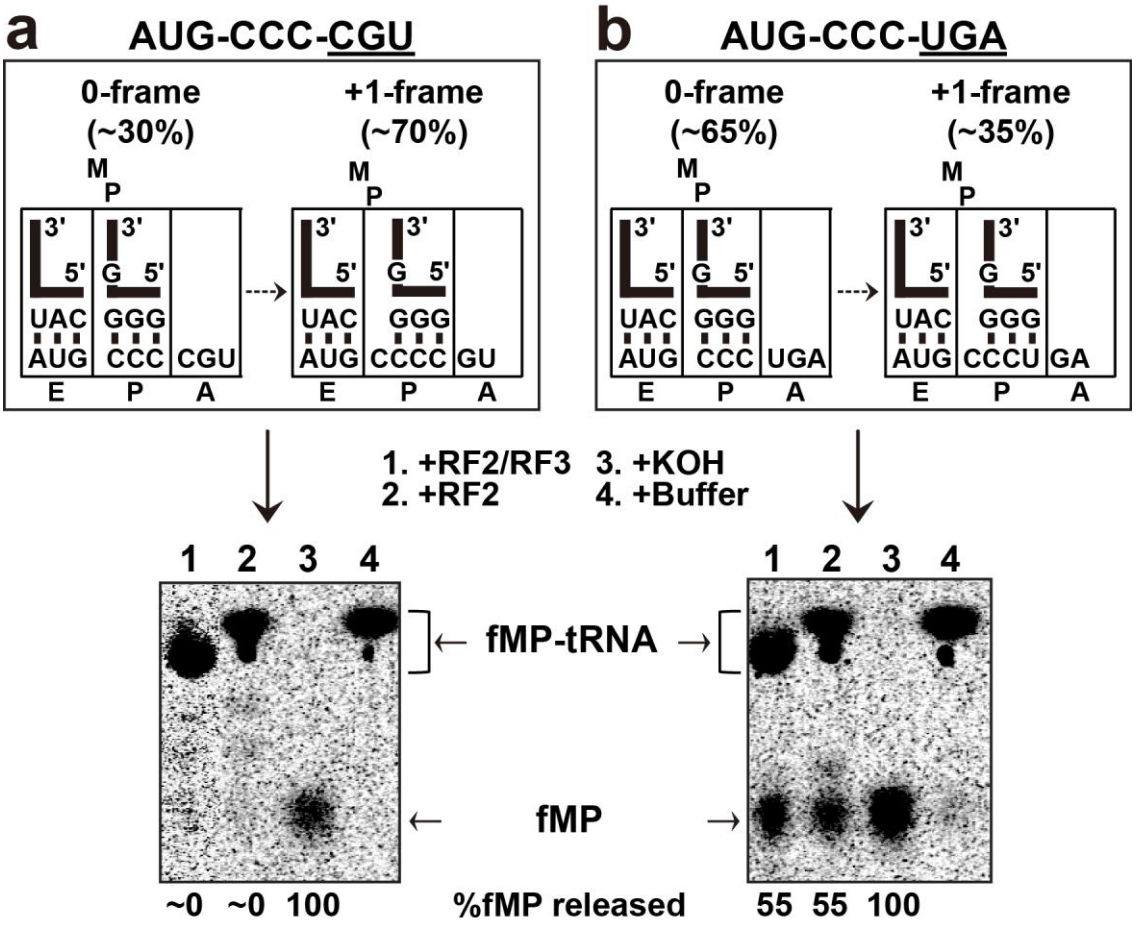

Supplementary Figure 8. Release factors do not recognize +1FS errors of tRNA$^{Pro/GGG}$.

Dipeptidyl-post-translocation complexes were formed by mixing the ternary complex of G37-state Pro-tRNA$^{Pro/GGG}$ and EF-G with a 70SIC programmed with **(a)** AUG-CCC-CGU (coding for fMPR) or **(b)** AUG-CCC-UGA (coding for fMP*, where * = stop). Both complexes were incubated 10 min at 37 °C to promote +1FS of P-site tRNA$^{Pro/GGG}$ at an expected frequency of ~70% on CCC-C (see Fig.2). Aliquots of each reaction were treated with (1) RF2 and RF3 (each 30 μM), (2) RF2 (30 μM), (3) KOH (0.8 M), or (4) the reaction buffer. Release of fMP was detected on electrophoretic TLC, where the signals at the origin represented a mixture of Met-tRNA^{fMet}, fMet-tRNA^{fMet}, and fMP-tRNA^{Pro}. The KOH treatment released all three acyl groups from tRNA, whereas RF2 released fMP only when tRNA^{Pro} was part of an authentic termination complex. The fractional release of fMP by each treatment relative to the KOH treatment was calculated

and listed below each lane in the phosphorimage. When the post-translocation complex contained a stop codon, release of fMP by RF2 was incomplete due in part to +1FS and in part to drop-off of fMP-tRNA^{Pro}. Failure to detect any RF2/RF3-mediated release of fMP indicates that, for GGG tRNA^{Pro}, +1FS errors are not recognized by the post-translocation quality control mechanism when base pairing is preserved in the codon-anticodon duplex. However, the post-translocation quality control may apply to UGG tRNA^{Pro}, because this tRNA will incur a mismatch in the codon-anticodon duplex.

Supplementary Figure 9.

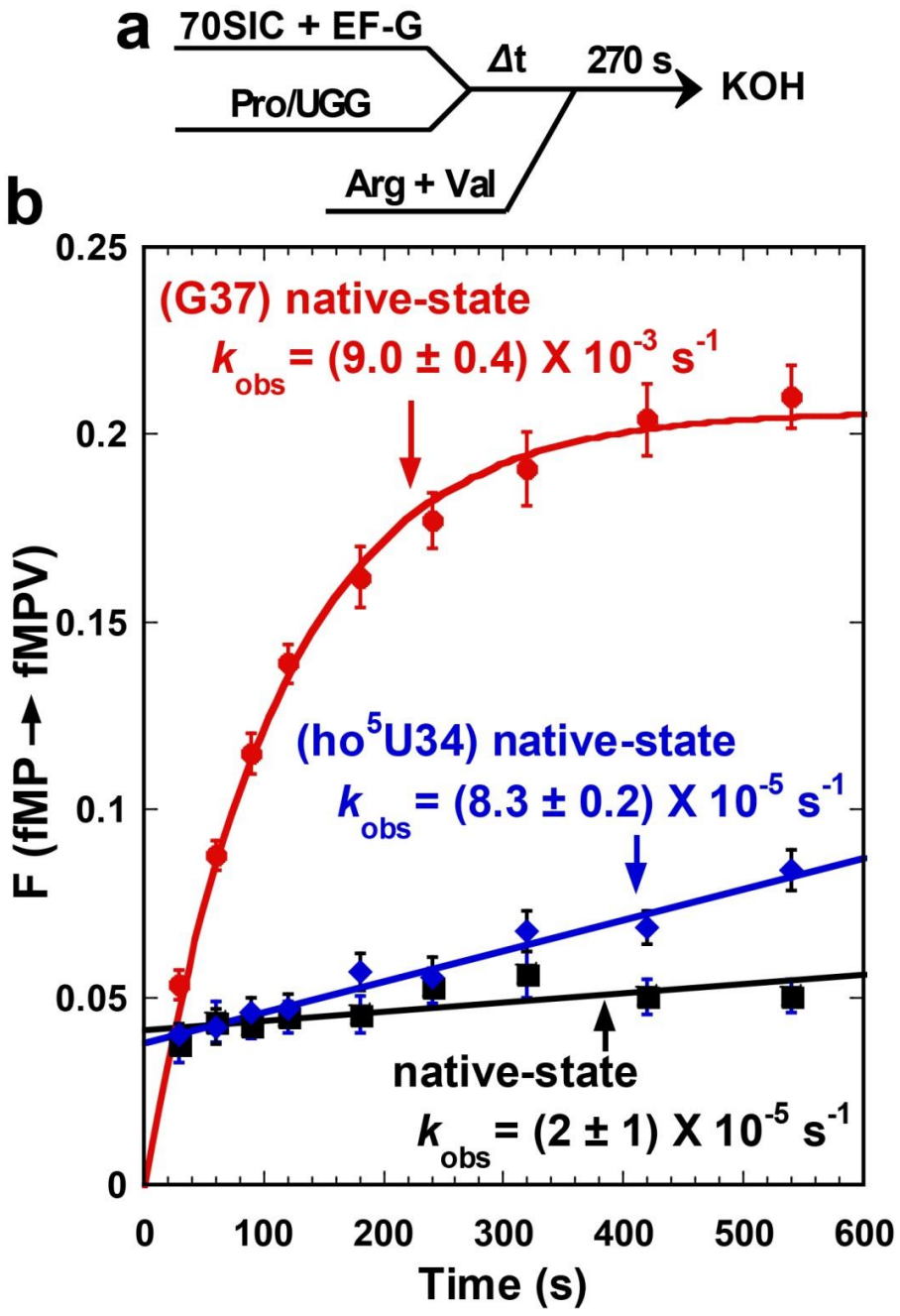

Supplementary Figure 9. The cmo^{5}U34 modification in tRNA$^{Pro/UGG}$ is not a major determinant for suppressing +1FS errors.

Native-state tRNA$^{Pro/UGG}$ contains cmo^{5}U34 and m^{1}G37 in the anticodon loop among other naturally occurring modifications. The fully modified native-state (the native-state) displays

background levels of +1FS errors, whereas the native-state lacking m^1G37 (the (G37) native-state) displays high levels of +1FS errors, indicating that m^1G37 is a major determinant of suppressing +1FS errors. In contrast, the (ho^5U34) native-state retained background levels of +1FS errors, indicating that the integrity of cmo^5U34 is not a determinant of suppressing +1FS errors. **a**. Kinetic scheme for monitoring +1FS errors. **b.** Kinetics of synthesis of fMPV, showing the rate constant and amplitude of +1FS product formation for the fully modified native-state, the (G37)-native state, and the (ho^5U34) native-state. The y-intercepts obtained with the native-state and the (ho^5U34) native-state tRNA are attributed to 4% slippage of $tRNA^{Pro/UGG}$ during translocation. The plot for the (G37) native-state does not resolve translocation-induced slippage, which was ~3% (see **Fig. 5f**). The (G37) native-state tRNA was purified from *ts-trmD-S88L* cells grown at 30 °C to OD_{600} of 0.4 and then shifted to 42 °C for 24 hrs[1], while the (ho^5U34) native-state tRNA was purified from *E. coli* cells deficient in the *cmoB* gene[4].

Supplementary Figure 10.

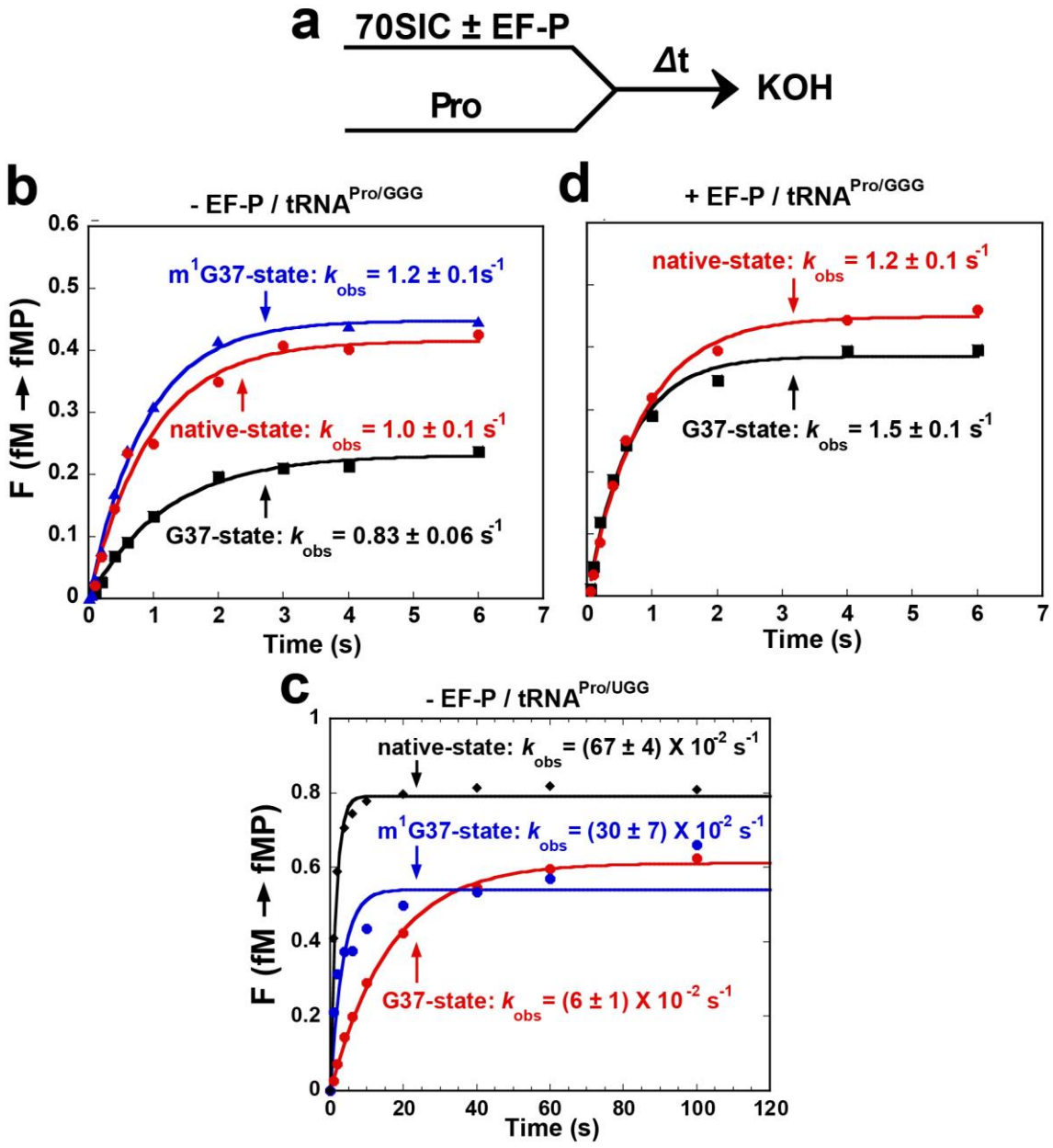

Supplementary Figure 10. Both m^{1}G37 and EF-P promote dipeptide formation.

a. Kinetic scheme for monitoring fMP formation from the 70SIC. **b.** and **c.** Increases in the rate of fMP formation by m^{1}G37- and native-state tRNA^{Pro} relative to the G37-state were observed for both tRNA$^{Pro/GGG}$ and tRNA$^{Pro/UGG}$. **d.** Addition of EF-P increased the rate of fMP formation by G37- and native-state tRNA$^{Pro/GGG}$ (compare **d** with **b**). The enhancements in these rates support earlier findings of the m^{1}G37 base[5] and EF-P[6].

Supplementary Figure 11.

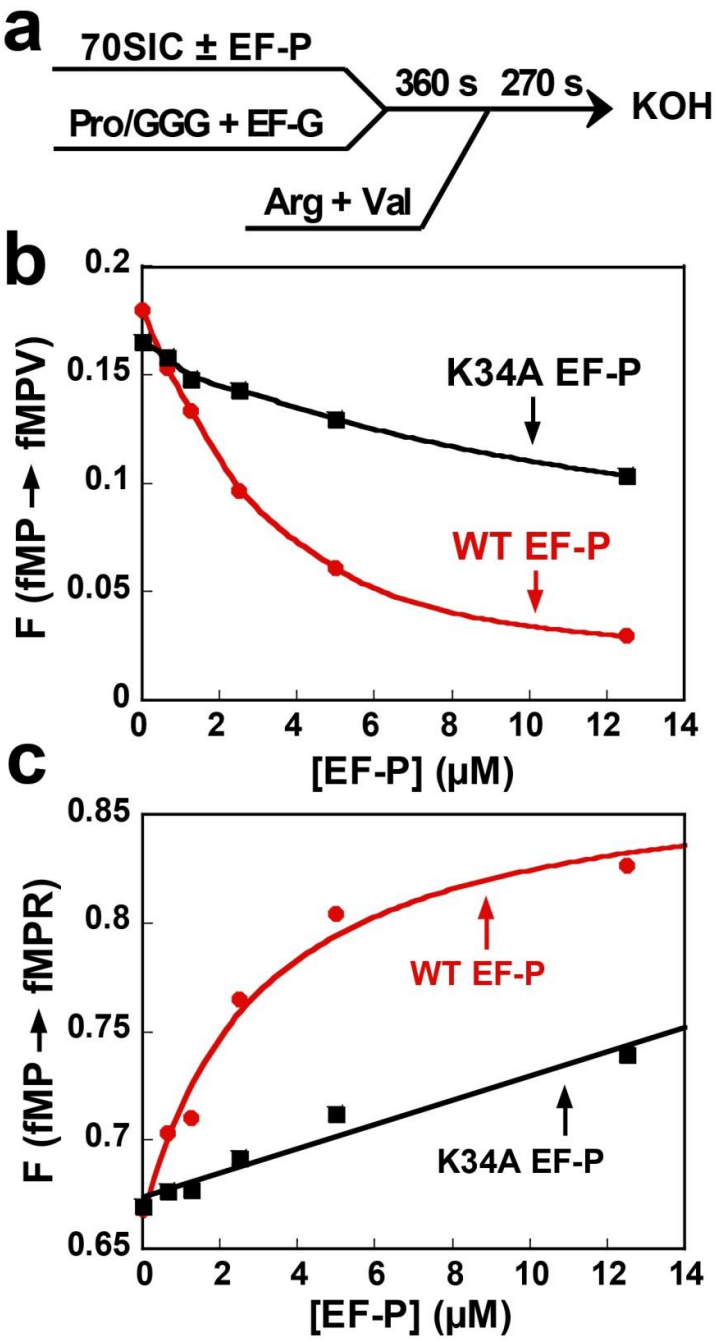

Supplementary Figure 11. Dependence of EF-P on the β-lysylation of K34 to suppress +1FS errors.

a. Reaction scheme for monitoring suppression of +1FS errors by EF-P. A 70SIC programmed with the AUG-CCC-CGU-U sequence was mixed with varying amounts of β-

lysinylated wild-type or K34A mutant EF-P and the ternary complex of G37-state $tRNA^{Pro}$ to rapidly form a stalled post-translocation complex in the presence of EF-G. After a delay of 360 s, peptide bond formation was initiated by addition of ternary complexes of $tRNA^{Arg}$ and $tRNA^{Val}$. Reactions were quenched with KOH and analyzed by electrophoretic TLC. **b.** Formation of +1-frame fMPV in the presence of wild-type (in red) or mutant (in black) EF-P. Inhibition of +1FS errors was correlated with enhanced synthesis of the in-frame product. **c**. Formation of in-frame fMPR in the presence of wild-type (in red) or mutant (in black) EF-P. Unmodified wild-type EF-P behaved similarly as the K34A mutant of EF-P (data not shown), indicating that the β-lysylation of K34 is a major determinant of error suppression.

Supplementary Figure 12.

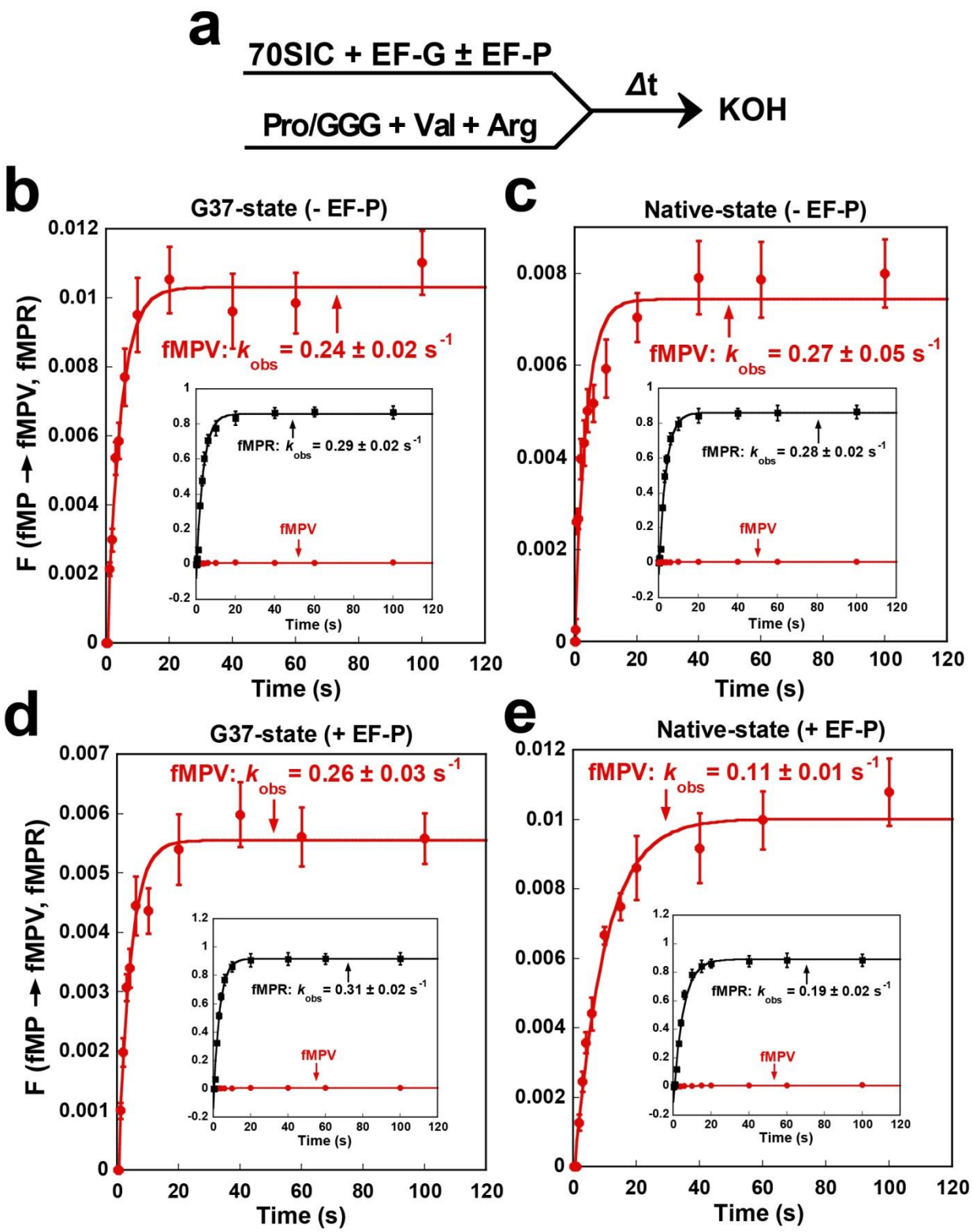

Supplementary Figure 12. Rapid +1FS of $tRNA^{Pro/GGG}$ during translocation to the P-site.

a. Kinetic scheme to monitor formation of fMPV and fMPR in the absence of ribosomal stalling. A 70SIC programmed with AUG-CCC-CGU-U was rapidly mixed with ternary complexes of the G37- or native-state $tRNA^{Pro/GGG}$ and ternary complexes of $tRNA^{Arg}$ and $tRNA^{Val}$ in the presence of EF-G. This design permitted decoding of the CCC triplet by $tRNA^{Pro}$ at the A-site, followed by peptide bond formation and translocation into the P-site, with the possibility to engage in +1-frame pairing before arrival at the P-site. Formation of fMPV and fMPR was monitored on electrophoretic TLC. **b-e.** Kinetics of tripeptide formation and associated rate constants are presented in the respective plots, showing G37-state $tRNA^{Pro}$ in the absence (**b**) or presence (**d**) of EF-P (10 µM) and native-state $tRNA^{Pro}$ in the absence (**c**) or presence (**e**) of EF-P (10 µM). While fMPR (in black, inset) and fMPV (in red) were formed at similar rates, the yield of fMPR relative to fMPV was approximately 100:1, indicating that the inclusion of the in-frame $tRNA^{Arg}$ did not block the rapid reaction of fMPV synthesis. Scatter in the data for fMPV prevented drawing conclusions about the effect of m^1G37 or EF-P on the frequency of +1FS.

Supplementary Figure 13.

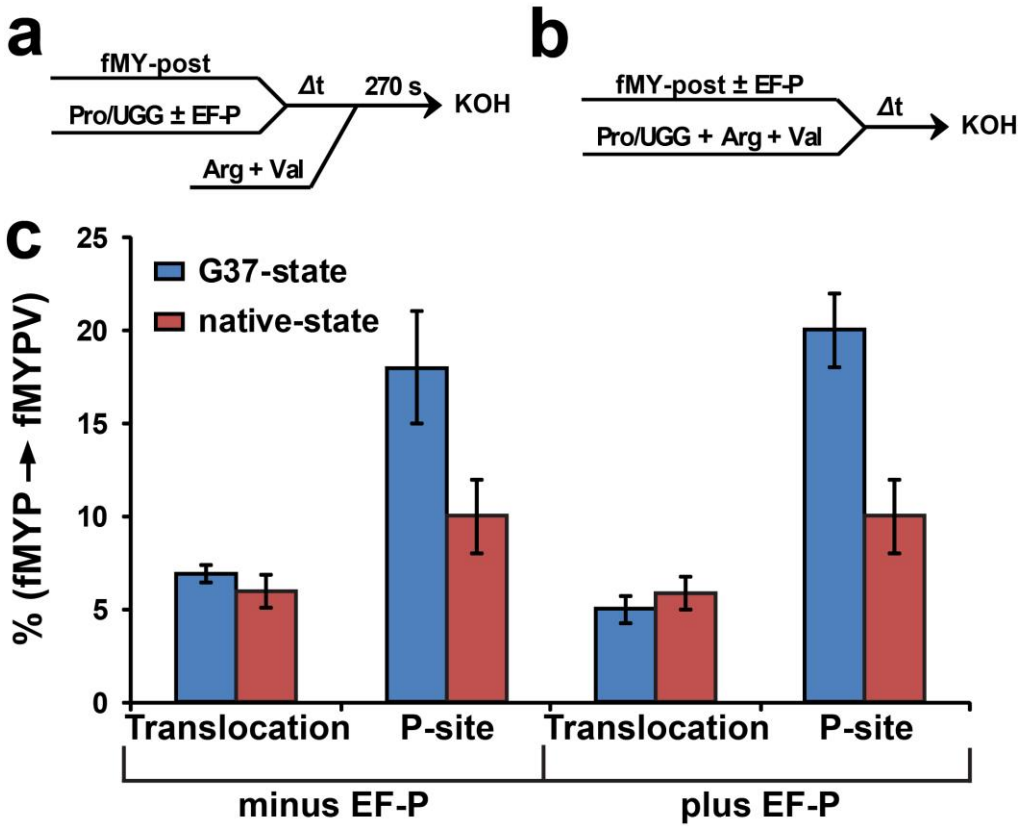

Supplementary Figure 13. Frequency of +1FS errors by G37- and native-state tRNA$^{Pro/UGG}$ when the CCC-C run is at the 3rd codon position.

The G37-state and the native-state tRNA$^{Pro/UGG}$ were evaluated for +1FS when translation was programmed with the AUG-UAU-CCC-CGU-U sequence in the presence or absence of EF-P. **a**. Kinetic scheme to monitor tRNA shifting from the P-site in a stalled post-translocation complex. **b**. Kinetic scheme to monitor tRNA shifting during translocation into the P-site. **c.** The extent of shifting during translocation and during P-site stalling is summarized in the bar graph, in which the fractional conversion of fMPY to fMYPV represents +1FS by tRNA$^{Pro/UGG}$. The extent of +1FS during translocation was determined directly from the one-step kinetic scheme, whereas the extent of +1FS during P-site stalling was obtained by subtracting translocation-induced +1FS from the level of +1FS observed after 500 s of P-site stalling. Values are the average of three independent measurements with error bars denoting SD.

Supplementary Table 1. Occurrence of CC[C/U]-[C/U] in *E. coli* K12 protein-coding genes (related to Supplementary Figure 1a).

Codon position	Number of CC[C/U]-[C/U]	Fraction (%)
1-15	393	16.7
16-100	1479	62.9
100-Stop	481	20.4
Total	2353	100.0

Supplementary Table 2. β-gal activity from *E. coli* with or without m^1G37 and EF-P, related to Figures 1b-1d.

a. Effect of m^1G37.

Position	m^1G37+	m^1G37-	-/+ Fold difference
2	1.0 ± 0.4	8.3 ± 0.6	8.0
5*	0.6 ± 0.2	1.7 ± 0.4	3.1
10*	0.6 ± 0.3	1.5 ± 0.8	2.4
20	0.5 ± 0.1	2.0 ± 0.8	4.4
60	0.6 ± 0.2	1.4 ± 0.5	2.5
124	0.4 ± 0.0	1.7 ± 0.6	4.0
124CGG	3.0 ± 0.2	4.4 ± 0.9	1.5
124UGG	1.7 ± 0.3	6.7 ± 0.6	4.0

b. Effect of EF-P.

Position	EF-P+	EF-P-	-/+ Fold difference
2	0.40 ± 0.03	1.23 ± 0.06	3.0
5*	0.43 ± 0.15	0.68 ± 0.07	1.6
10*	0.17 ± 0.01	0.29 ± 0.10	1.7
20	0.13 ± 0.01	0.25 ± 0.02	1.9
60	0.06 ± 0.03	0.08 ± 0.01	1.3
124	0.06 ± 0.01	0.08 ± 0.04	1.3
124CGG	0.14 ± 0.01	0.34 ± 0.01	2.4
124UGG	0.13 ± 0.02	0.48 ± 0.02	3.6

c. Effect of K34A EF-P.

Position	+ WT EF-P	+ K34A EF-P	-/+ Fold difference
2	0.49 ± 0.08	1.85 ± 0.16	3.8
10*	0.14 ± 0.01	0.63 ± 0.23	4.6

The symbol * denotes that the CCC constructs for calculation of +1FS frequency at the 5th and 10th positions were not available. For these two positions, the value of the CCC constructs was taken from the average value measured at the 2nd, 20th, 60th and 124th positions. The SD (standard deviation) was usually ≤ 10% of the average.

Supplementary Table 3. Summary of kinetic data.

a. +1FS errors of $tRNA^{Pro/GGG}$ during the 1st round of elongation at CCC-C*.

$tRNA^{Pro/GGG}$	+1FS	minus EF-P		plus EF-P	
		Translocation	P-site	Translocation	P-site
G37-state transcript	frequency (%)	1.0 ± 0.1	15 ± 2	0.55 ± 0.06	2.6 ± 0.7
	k_{obs} (s^{-1})	(2.4 ± 0.2) X 10^{-1}	(2.0 ± 0.3) X 10^{-3}	(2.6 ± 0.3) X 10^{-1}	(5.3 ± 0.1) X 10^{-5}
native-state	frequency (%)	0.7 ± 0.2	7.4 ± 0.3	1.0 ± 0.2	2.9 ± 0.4
	k_{obs} (s^{-1})	(2.7 ± 0.5) X 10^{-1}	(1.3 ± 0.1) X 10^{-2}	(1.1 ± 0.1) X 10^{-1}	(6.3 ± 0.1) X 10^{-5}

b. +1FS errors of $tRNA^{Pro/UGG}$ during the 1st round of elongation at CCC-C*.

$tRNA^{Pro/UGG}$	+1FS	minus EF-P		plus EF-P	
		Translocation	P-site	Translocation	P-site
G37-state transcript	frequency (%)	5.9 ± 0.3	28 ± 1	2.8 ± 0.1	16 ± 1
	k_{obs} (s^{-1})	(6 ± 1) X 10^{-2}	(4.8 ± 0.2) X 10^{-3}		(2.9 ± 0.3) X 10^{-3}
m^1G37-state transcript	frequency (%)	3.0 ± 0.6	2.1 ± 0.7	2.7 ± 0.2	2.7 ± 0.3
	k_{obs} (s^{-1})	(3.0 ± 0.6) X 10^{-2}	(4.7 ± 0.5) X 10^{-5}		(6.7 ± 0.3) X 10^{-5}
native-state	frequency (%)	2.5 ± 0.4	2.5 ± 0.6	2.1 ± 0.1	0.5 ± 0.3
	k_{obs} (s^{-1})	>10^{-2}	(2 ± 1) X 10^{-5}		(2 ± 1) X 10^{-5}

c. +1FS errors of $tRNA^{Pro/GGG}$ in the P-site of a stalled fMYP-post-translocation complex*.

$tRNA^{Pro}$	+1FS	GGG isoacceptor		UGG isoacceptor	
		minus EF-P	plus EF-P	minus EF-P	plus EF-P
G37-state transcript	extent (%)	43 ± 1	34 ± 2	18 ± 3	20 ± 2
	k_{obs} (s^{-1})	(1.9 ± 0.2) X 10^{-2}	(7.0 ± 1) X 10^{-3}		(2.2 ± 0.7) X 10^{-4}

*The rate (s^{-1}) and frequency (%) of +1FS associated with translocation were indirectly monitored by measuring the fraction of fMP converted to fMPV in a concerted reaction started

by mixing 70SIC with ternary complexes of $tRNA^{Pro}$, $tRNA^{Arg}$, and $tRNA^{Val}$ in the presence of EF-G. The rate of +1FS of fMP-$tRNA^{Pro}$ or fMYP-$tRNA^{Pro}$ in the P-site of a stalled post-translocation complex was measured using a two-step reaction in which timed aliquots of freshly prepared post-translocation complex were mixed over time with ternary complexes of $tRNA^{Arg}$ and $tRNA^{Val}$ to form 0-frame and +1-frame tripeptides. The frequency of +1FS within the P-site was determined by subtracting the value for +1FS obtained from the one-step protocol from the value for +1FS obtained from the two-step protocol (after a stall time of 500 s).

Supplementary References

1. Masuda, I., Sakaguchi, R., Liu, C., Gamper, H. & Hou, Y.M. The Temperature Sensitivity of a Mutation in the Essential tRNA Modification Enzyme tRNA Methyltransferase D (TrmD). *J Biol Chem* **288**, 28987-96 (2013).
2. Mitchell, S.F. et al. The 5'-7-methylguanosine cap on eukaryotic mRNAs serves both to stimulate canonical translation initiation and to block an alternative pathway. *Mol Cell* **39**, 950-62 (2010).
3. Kothe, U. & Rodnina, M.V. Codon reading by tRNAAla with modified uridine in the wobble position. *Mol Cell* **25**, 167-74 (2007).
4. Kim, J. et al. Structure-guided discovery of the metabolite carboxy-SAM that modulates tRNA function. *Nature* **498**, 123-6 (2013).
5. Bjork, G.R. & Nilsson, K. 1-methylguanosine-deficient tRNA of Salmonella enterica serovar Typhimurium affects thiamine metabolism. *J Bacteriol* **185**, 750-9 (2003).
6. Glick, B.R. & Ganoza, M.C. Identification of a soluble protein that stimulates peptide bond synthesis. *Proc Natl Acad Sci U S A* **72**, 4257-60 (1975).